PAV-88-02

Transient Effects in Low-Temperature-Induced Fracture and Failure of Pavement Structures

Ontario

Ministry of Transportation

Research and Development Branch

89-03212/

Technical Report Documentation Page

Transient Effects in Low-Temperature-Induced Fracture and Failure of Pavement

Authors:	A.P.S. Selvadurai, Professor and Chairman and M.C. Au, Post-Doctoral Fellow, Department of Civil Engineering, Carleton University
Number:	PAV-88-02
Date of Publication:	December 1988
Published by:	Research and Development Branch, MTO
Ministry Contact:	Gerhard Kennepohl (416) 235-4701
Abstract:	This report focuses on the development of a numerical method of transient stress analysis of a pavement structure which is subjected to heat conduction and associated thermoelastic effects. The numerical analysis of the problem is based on a finite element modelling which takes into account the time-dependent fluctuations of the surface temperature of the pavement structure. The pavement structure is composed of a surface layer of a compacted base and sub-base in which the thickness, mechanical properties and the thermal properties can be assigned suitable values available in the literature. The stress analysis technique can accommodate the existence of cracks either within the surface layer, at the interface between the surface layer and the base courses, or at the interface between the base layer and the sub-base. The numerical modelling can also examine the influence of reinforcing layers which are placed at cracked locations to prevent reflection cracking in an overlay. The stress analysis technique develops solutions for plausible models for the initiation of failure within intact pavements which are subjected to low-temperature effects. In the case of pavement structures containing surface flaws, the stress analysis develops results which indicate the manner in which the stress intensity factors or fracture toughness measures vary due to abrupt temperature fluctuations. The report also presents studies which examine the efficiency of reinforcing layers in their ability to suppress the development of reflecting cracking in new overlays.
Comments:	Final report of the Research and Development Branch, Project 21159
Key Words:	low-temperature cracking, stress analysis, finite element modelling, asphalt pavements, layer reinforcement
Distribution:	MTO Head Office and Regions, Municipalities and other highway agencies
Copyright Status:	Crown copyright © 1988 Ministry of Transportation

PAV-88-02

Transient Effects in Low-Temperature-Induced Fracture and Failure of Pavement Structures

A.P.S. Selvadurai
Professor and Chairman

M.C. Au
Post-Doctoral Fellow

Department of Civil Engineering
Carleton University

Published by
The Research and Development Branch
Ontario Ministry of Transportation
Hon. Ed Fulton, Minister
D.G. Hobbs, Deputy Minister

Published without prejudice as to the application of the findings.
Crown copyright reserved; however, this document may be reproduced for non-commercial purposes with attribution to the Ministry.

For additional copies, contact:
The Editor, Technical Publications
Room 320, Central Building
1201 Wilson Avenue
Downsview, Ontario
Canada M3M 1J8

Telephone: (416) 235-3480
CNCP Dialcom Electronic Mail: 23:MIN006

December 1988

Table of Contents

Acknowledgements iii

1/ Introduction 1

2/ Fundamental Equations 4

3/ Finite Element Modelling

3.1/ The Galerkin Formulation 6

3.2/ The Effects of Reinforcement 9

4/ Time Integration and Iterative Schemes 11

5/ Failure and Fracture Concepts 13

6/ Modelling of Low-Temperature-Induced Failure 16

7/ Modelling of Low-Temperature-Induced Fracture-Effect of a Reinforcing Layer 17

8/ Modelling of Low-Temperature-Induced Fracture-Effect of Interface Characteristics 19

9/ Conclusions 21

10/ References 23

I. ACKNOWLEDGEMENTS

The work presented in this report was carried out under the Ministry of Transportation of the Province of Ontario as Research Project No.21159. The authors wish to express their gratitude to Mr. W.A. Phang, Head, Research and Development Branch, Pavement and Roadway Office, for his valuable advice in all phases of the development of the conceptual models.

1 INTRODUCTION

The evaluation and prediction of the performance of asphalt pavement structures which are subjected to low-temperature effects is of fundamental importance to efficient pavement design. In this regard, the subject of low-temperature cracking of asphalt pavements has received concerted attention over the past three decades. Recent initiatives in terms of the comprehensive assessment of factors influencing low-temperature-induced transverse cracking are summarized in an Asphalt Institute Research Report [1]. The International Conferences [2,3] on Paving in Cold Areas also document recent advances in the modelling, design, field investigation, and laboratory observations pertaining to the initiation and propagation of low-temperature-induced transverse cracking of asphalt pavements. Since the references [1-3] contain extensive accounts of literature pertaining to the subject, no attempt will be made to provide a comprehensive bibliography.

When asphalt pavements are subjected to sudden cooling by air temperature, thermal stresses can develop in the various asphalt layers. The degree to which such stresses can manifest depends on the degree of restraint offered by the various components of the pavement structure. The thermal stresses induced within a pavement structure can disappear with time in situations where the asphalt exhibits stress relaxation phenomena. In the low temperature range, however, the temperature-induced stresses, in general, will not diminish. The contact conditions between the asphalt layer and the base will resist the contractive deformations, resulting in the development of tensile stresses within the asphalt layer. The physical condition and the thermo-mechanical properties of the asphalt layer will then govern the development of low-temperature cracking of the layer [4]. The low-temperature performance of a pavement structure can be influenced by a variety of factors. Some of the factors which exert a dominant influence on the process of transverse crack initiation and its subsequent propagation can be classified as follows:

(a) the initial condition of the pavement, defined in terms of the density, porosity, permeability achieved in the in-situ compacted state, and degree of damage, in terms of micro cracks, that may be induced during the compaction process;

(b) the thermo-mechanical properties of the separate phases (i.e., asphalt and aggregates) constituting the asphalt mixture, defined in terms of the thermal expansion/contraction properties, heat conduction characteristics, temperature-dependent elasticity, viscoelasticity, creep, and strength characteristics of the separate phases;

(c) the thermo-mechanical properties of the subgrade materials, defined in terms of the heat transfer, moisture transfer, and temperature-dependent deformability characteristics of the subgrade materials;

(d) the thermo-mechanical properties of the asphalt composite, defined in terms of thermal expansion/contraction properties, heat conduction characteristics, temperature-

dependent elasticity, viscoelasticity, creep, and strength characteristics of the compacted asphalt;

(e) the thermo-mechanical properties of the interfaces, defined in terms of elasticity, creep, and frictional and strength characteristics of the various interfaces encountered in the pavement structure;

(f) transient thermal effects, defined in terms of daily or seasonal variations (especially rates of change) in the surface temperature of the pavement structure;

(g) transient loading effects, defined in terms of loading patterns consistent with traffic-induced static and dynamic loads;

(h) degradation phenomena, defined in terms of cracking in the asphalt pavement structure, delamination at the asphalt-layer/sub-base interface, embrittlement of the asphalt, etc..

A rigorous treatment of all of the above factors, with a view to predicting the time- and temperature-dependent occurrence and propagation of transverse cracking in an asphalt layer, is an extremely difficult task. Even if the mathematical modelling of the process involved can be fulfilled, the determination of specific material functions which are required for such models presents a complicated exercise in materials testing. Prior to considering such comprehensive and all-encompassing models which attempt to predict transverse cracking phenomena, it is instructive to identify certain plausible elementary models which contain salient features which promote either the development of failure in an intact asphalt layer or the propagation of existing flaws in a damaged asphalt layer.

This report focuses on the transient stress analysis of a pavement structure which is subjected to heat conduction and associated thermo elastic effects. Thermoelastic modelling of the asphalt pavement is, of course, a relatively elementary model of the thermo-mechanical behaviour of asphalt materials which are subjected to the range of temperatures encountered in a pavement structure, especially leading to the low-temperature environment. It is meant to serve as a preliminary study which will be extended, in future investigations, to accommodate complete thermo-viscoelastic or thermo-visco-plastic constitutive responses. The numerical analysis of the transient thermo-elastic effects is performed by appeal to the finite element method. Transient effects occur by virtue of time-dependent temperature fluctuations at the surface of the pavement structure. The failure initiation can be predicted via a simplified maximum stress criterion applicable to the asphalt layer. In the modelling of damaged pavement, account is taken of surface cracks, delaminations, etc., that are present in the surface asphalt layer and at the interfaces respectively. The numerical analysis of the damaged pavement focuses on the evaluation of the time-dependent stress intensity factor(s) at the crack tip. This is a measure of the energy that can be

released while propagating the crack further. The fracture criterion for the propagation of the crack can be assessed in relation to a critical stress intensity factor derived via experimental means. At critical conditions, the stress intensity factor is a measure of the fracture toughness of the material.

2 FUNDAMENTAL EQUATIONS

We consider the class of classical coupled-thermoelastic problems which have been treated quite extensively in the literature in solid mechanics [5,6]. The displacement equations of equilibrium governing the thermoelastic problem for a region D are given by:

$$(\lambda+\mu)u_{\ell,\ell i}+\mu u_{i,\ell\ell}-\beta T_{,i}=\rho\ddot{u}_i \quad ; \quad x_i \epsilon D \tag{1}$$

where λ and μ are the isothermal values of Lame's constants, β is the thermoelastic coefficient, ρ is the mass density, and u_i and T are respectively the unknown displacement and temperature fields which are functions of position (x_i) and time (t). The subscripts indicate directions x, y, z (1, 2, 3), and repeated indices are summed over the range of subscripts. The dot indicates a time derivative and a comma indicates a partial derivative with respect to the spatial variables. The general heat conduction equation, which includes the heat source (or sink) term due to a mechanical effect, can be written as:

$$(kT_{,i})_{,i}-\rho c\dot{T}-T_o\beta\dot{\epsilon}_{\ell\ell}+Q=0 \quad ; \quad x_i \epsilon D \tag{2}$$

where k is the coefficient of thermal conductivity, c is the specific heat, Q is the heat source term other than mechanical effect, and T_o is the initial temperature distribution when the medium is unstrained. The linearized strain tensor is defined by:

$$\epsilon_{ij}=\frac{1}{2}(u_{i,j}+u_{j,i}) \tag{3}$$

and the linear thermoelastic stress-strain relationship takes the form:

$$\sigma_{ij}=C_{ijk\ell}\epsilon_{k\ell}-\beta(T-T_o)\delta_{ij} \tag{4}$$

where δ_{ij} is Kronecker's delta function. In situations where the mechanical deformations induce little change in temperature of the body, the thermoelastic term in (2) is zero; i.e., $(T-T_o)\beta\dot{\epsilon}_{\ell\ell}=0$. We shall also restrict our attention to the class of quasi-static thermoelastic problem in which the inertia term in (1) can be neglected; i.e., $\rho\ddot{u}_i=0$.

The reduced forms of the governing differential equations (1) and (2) are subjected to the following boundary and initial conditions. The boundary conditions for the heat conduction problem are:

$$T = \overline{T} \quad \text{on } x_i \epsilon S_1 \tag{5}$$

$$k\frac{\partial T}{\partial \underset{\sim}{n}} = \overline{q} \quad \text{on } x_i \epsilon S_2 \tag{6}$$

where $\overline{T}$ is the value of the temperature on the surface S_1, $\overline{q}$ is the rate of heat loss at the boundary S_2, $\underset{\sim}{n}$ is the outward unit normal to S_2, and $S_1 U S_2$ corresponds to the surface S of D.

For the elastic problem, the boundary conditions are:

$$u_i = \overline{u}_i \quad \text{on } x_i \epsilon S_3 \tag{7}$$

$$\sigma_{ij} n_j = \overline{P}_i \quad \text{on } x_i \epsilon S_4 \tag{8}$$

where $\overline{u}_i$ corresponds to the boundary displacement on S_3, $\overline{P}_i$ are the boundary tractions on S_4, and $S_3 U S_4$ corresponds to the surface S of D. The initial temperature in the body is set equal to T_o. Also, the parameter β can be expressed in terms of the isotropic elastic constants λ, μ, and the coefficient of thermal expansion as:

$$\beta = (3\lambda + 2\mu)\alpha. \tag{9}$$

3 FINITE ELEMENT MODELLING

The solution of the equations of transient thermoelasticity described in Section 2 can be approached in a variety of ways. These include analytical methods based on integral transform techniques and numerical methods based on finite difference, finite element, and boundary integral equation techniques. In view of the finite geometries associated with the modelling of the pavement structures and the crack regions present in such regions, it is convenient to adopt a numerical method of stress analysis which is based on a finite element formulation. In particular, a Galerkin finite element technique is adopted in the development of the numerical procedures.

3.1 The Galerkin Formulation

In the quasi-static thermoelastic problem, the thermal and the elastic problems can be considered independently. Therefore, δT and δu_i can be considered as the variation functions, for the problem defined in the previous section, and the corresponding Galerkin expressions can be written as:

$$\int_D \delta T \left[(kT_{,i})_{,i} - \rho c T \right] dD = \int_{S_2} \delta T \left(k \frac{\partial T}{\partial n} - \overline{q} \right) dS \tag{10}$$

and

$$\int_D \delta u_i \left(\sigma_{ij,j} - b_i \right) dD = \int_{S_4} \delta u_i \left(P_i - \overline{P}_i \right) dS \tag{11}$$

respectively. Integrating by parts once the first term of (10) and (11), we obtain:

$$\int_D \left[k \delta T_{,i} T_{,i} + \rho c \delta T \dot{T} \right] dD - \int_{S_2} \delta T \overline{q} dS = 0 \tag{12}$$

and

$$\int_D \left[\delta \epsilon_{ij} \sigma_{ij} + \delta u_i b_i \right] dD - \int_{S_4} \delta u_i \overline{P}_i dS = 0 \tag{13}$$

For an isotropic elastic material, we note that $C_{ij\ell m} = (\lambda \delta_{ij} \delta_{\ell m} + \mu \delta_{i\ell} \delta_{jm} + \mu \delta_{im} \delta_{j\ell})$ and (13) can be written as:

$$\int_D \left[\delta\epsilon_{ij} C_{ijlm} \epsilon_{lm} + \delta u_i b_i + \delta\epsilon_{ij}\beta\left(T - T_o\right)\delta_{ij}\right] dD - \int_{S_4} \delta u_i \overline{P}_i dS = 0 \tag{14}$$

Equations (12) and (14) are the required variational expression for the finite element discretization. Consequently, they can be written in a discretized form as:

$$\sum_e \left\{ \int_{F_e} \left[k\delta T_{,i} T_{,i} + \rho c \delta T \dot{T}\right] dD - \int_{F_e \bigcap S_2} \delta T \overline{q} dS \right\} = 0 \tag{15}$$

and

$$\sum_e \left\{ \int_{F_e} \left[\delta\epsilon_{ij} C_{ijlm} \epsilon_{lm} + \delta u_i b_i + \delta\epsilon_{ij}\beta(T - T_o)\delta_{ij}\right] dD - \int_{F_e \bigcap S_4} \delta u_i \overline{P}_i dS \right\} = 0 \tag{16}$$

respectively, where F_e is an element such that:

$$D = \sum_e F_e \tag{17}$$

For the two-dimensional problem, one can use the following representations:

$$T = [N_T]\{T\}_e^n \tag{18}$$

$$\begin{bmatrix} u_x \\ u_y \end{bmatrix} = \begin{bmatrix} N_u & 0 \\ 0 & N_u \end{bmatrix} \begin{bmatrix} u_x \\ u_y \end{bmatrix}_e^n \tag{19}$$

$$\begin{bmatrix} \frac{\partial T}{\partial x} \\ \frac{\partial T}{\partial y} \end{bmatrix} = \begin{bmatrix} \frac{\partial N_T}{\partial x} \\ \frac{\partial N_T}{\partial y} \end{bmatrix} \{T\}_e^n = \begin{bmatrix} B_{Tx} \\ B_{Ty} \end{bmatrix} \{T\}_e^n \tag{20}$$

and

$$\begin{bmatrix} \epsilon_{xx} \\ \epsilon_{yy} \\ \epsilon_{xy} \end{bmatrix} = \begin{bmatrix} \frac{\partial N_u}{\partial x} & 0 \\ 0 & \frac{\partial N_u}{\partial y} \\ \frac{\partial N_u}{\partial y} & \frac{\partial N_u}{\partial x} \end{bmatrix} \begin{bmatrix} u_x \\ u_y \end{bmatrix}_e^n = \begin{bmatrix} B_{ux} & 0 \\ 0 & B_{uy} \\ B_{uy} & B_{ux} \end{bmatrix} \begin{bmatrix} u_x \\ u_y \end{bmatrix}_e^n \tag{21}$$

(15) and (16) can be written as:

$$\sum_e \{\delta T\}_e^{*n} \left[[K_{TT}^e] \{T\}_e^n + [M_{TT}]^e \left\{\dot{T}\right\}_e^n - \{P_T\}_e^n \right] = 0 \tag{22}$$

and

$$\sum_e \begin{bmatrix} \delta u_x \\ \\ \delta u_y \end{bmatrix}_e^{*n} [[K_{uu}^e] \{u\}_e^n + [K_{uT}^e] [\{T\}_e^n - \{T_o\}_e^n] - \{P_u\}_e^n] = 0 \tag{23}$$

respectively. Also, $\{\ \}^*$ indicates the transpose of the matrix. After summation and considering the variations, we obtain:

$$[K_{TT}] \{T\} + [M_{TT}] \{\dot{T}\} = \{P_T\} \tag{24}$$

and

$$[K_{uu}] \{U\} + [K_{uT}] \{T\} = \{P_u\} \tag{25}$$

where the global matrices are:

$$[[K_{TT}] \quad ; \quad [K_{uu}] \ ; \ [M_{TT}] \ ; \ [K_{uT}] \ ; \ \{P_T\} \ ; \ \{P_u\}]$$

$$= \sum_e [[K_{TT}^e] \ ; \ [K_{uu}^e] \ ; \ [M_{TT}^e] \ ; \ [K_{uT}^e] \ ; \ \{P_T\}_e^n \ ; \ \{P_u\}_e^n] \tag{26}$$

The element matrices and vectors are:

$$[K_{TT}^e] = \int_{F_e} k [B_T]^* [B_T] \, dD \tag{27}$$

$$[K_{uu}^e] = \int_{F_e} [B_u]^* [C] [B_u] \, dD \tag{28}$$

$$[M^e_{TT}] = \int_{F_e} \rho c \, [N_T]^* \, [N_T] \, dD \tag{29}$$

$$[K^e_{uT}] = \int_{F_e} \beta \left[\overline{B}_u\right]^* [N_T] \, dD \tag{30}$$

$$\{P^e_T\} = \int_{F_e \bigcap S_2} [N_T]^* \, \bar{q} ds \tag{31}$$

and

$$\{P^e_u\} = \int_{F_e \bigcap S_4} [N_u]^* \left\{\overline{P}\right\} ds - \int_{F_e} [N_u]^* \{b\} dD \tag{32}$$

where

$$\left[\overline{B}_u\right] = \begin{bmatrix} B_{ux} \\ B_{uy} \end{bmatrix} \tag{33}$$

3.2 The Effects of Reinforcement

In this study, we shall also examine the type of problem in which the pavement structures are reinforced with a single layer of reinforcing material. The reinforcing elements are modelled as one-dimensional elements which possess axial stiffness. The element stiffness matrices $[M^e_{TT}]$, $[K^e_{TT}]$, and $[K^e_{uu}]$ for the one-dimensional elements take the forms:

$$[M^e_{TT}] = \rho c \begin{bmatrix} 2 & 1 \\ 1 & 2 \end{bmatrix} \tag{34}$$

$$[K^e_{TT}] = k \begin{bmatrix} 1 & -1 \\ -1 & 1 \end{bmatrix} \tag{35}$$

and

$$[K^e_{uu}] = \frac{EA}{\ell} \begin{bmatrix} a & b & -a & -b \\ & c & -b & -c \\ sym. & & a & b \\ & & & c \end{bmatrix} \tag{36}$$

where EA/ℓ is the axial stiffness of the reinforcing members and:

$$a = \cos^2\theta, \quad b = \cos\theta \sin\theta, \quad \textit{and} \quad c = \sin^2\theta \tag{37}$$

In (37), θ is the angle of the reinforcement with respect to the x-axis.

4 TIME INTEGRATION AND ITERATIVE SCHEMES

In order to obtain the recurrence relations for the time domain of equation (24), we can apply the scheme proposed by Zienkiewicz [7]:

$$\{T\} = [\{T_{t+\Delta t}\} - \{T_t\}] / \Delta t \tag{38}$$

and

$$\{T\} = (1 - f)\{T_t\} + f\{T_{t+\Delta t}\} \tag{39}$$

where Δt is a time step and f is the weighting factor such that $0 < f < 1$. Therefore, equation (24) can be expressed as:

$$[[M_{TT}] + f\Delta t[K_{TT}]]\{T_{t+\Delta t}\} = \{P_t\}\Delta t - [[M_{TT}] + (1 - f)\Delta t[K_{TT}]]\{T_t\} \tag{40}$$

The general expression for the equilibrium equation can be written as:

$$[K_{uu}]\{u_{t+\Delta t}\}^{i+1} = \{P_u\} - [K_{uT}]\{T_{t+\Delta t}\}^i \tag{41}$$

where i is the iteration number. An example for the need for iterating (41) is the possibility of separation at the interface of two different materials. The implementation of the separation model is as follows:

(Step 1): Along the expected path of separation (the interface), double nodes are used on either side of the interface.

(Step 2): The double nodes pair as connected by the reinforcing element defined by equations (34) to (37) of Section 3.2.

(Step 3): After a thermoelastic analysis of the problem at a given time-step, the tensile stresses of the reinforcing element are calculated and are compared to a tensile criterion of the reinforcing material. The criterion can be obtained by the tensile strength of the reinforcement or by pre-compressive stress within the elastic medium (for example, self-weight effects).

(Step 4): If the criterion of the separation is reached by certain elements, the corresponding EA/ℓ values in (36) will be set to zero, and (41) is re-calculated until a stable configuration is obtained.

(Step 5): If no element reaches the separation criterion, the computation of the strain and stress of the elastic medium is carried out; that is:

$$\{\epsilon\} = [B_u]\,\{u\}_e^n \tag{42}$$

and

$$\{\sigma\} = [C]\,[B_u]\,\{u\}_e^n - \beta\left[\overline{N}_T\right]\{T\}_e^n \tag{43}$$

where

$$\left[\overline{N}_T\right] = \begin{bmatrix} N_T \\ N_T \\ 0 \end{bmatrix} \tag{44}$$

Step(6): If no other results are required, the computation will be advanced to the new time-step.

5 FAILURE AND FRACTURE CONCEPTS

The transient thermoeleastic stress analysis technique and the associated numerical developments presented earlier can be used to examine the initiation of failure and fracture in the asphalt layer of a composite pavement structure. Attention is restricted to the occurrence of low temperature induced failure and fracture in a two-dimensional configuration of the pavement which exhibits a state of generalized plane strain. The condition relating to the occurrence of failure is prescribed by a maximum tensile stress criterion. According to such a criterion failure is assumed to occur when the in-plane tensile stresses within a location in the pavement reaches a certain critical tensile stress σ_o. In this study the value of σ_o is assumed to be independent of the temperature. The analysis can be easily modified to account for any prescribed variation of the critical tensile stress with temperature [1]. The numerical analysis scheme accounts for the separation of material surfaces in the failed region so that no material resistance is realized in a failed region. An iterative scheme is employed in such computations.

When flaws are present in the asphalt pavement the conditions which cause such flaws to propagate, in a brittle fashion, can be determined by appeal to linear thermo-elastic fracture mechanics. Fracture mechanics concept introduces, by analytical considerations, the magnitude and distribution of the stresses around the crack tip of an idealized crack, as a function of the crack size, the elastic properties of the material and a parameter referred to as a stress intensity factor (K). The stress intensity factor accounts for the manner in which the crack affects the state of stress at the crack tip. The magnitude of K reflects the state of stress associated with the mode of loading of the crack. For a state of plane strain, two modes of fracture can be identified. That associated with the flaw opening mode (K_I) and the in-plane flaw shearing mode (K_{II}). The criteria for the propagation of the crack can be assigned by considering the critical values of the stress intensity factors (K_I^c *and* K_{II}^c) individually or in a mixed mode. The critical values of the stress intensity factors are directly related to the fracture toughness of the material in the respective modes. Also as shown by Sih and Liebowitz [8] the classical solution for the elastic displacement field in the vicinity of a crack-tip as shown in Figure (1) can be expressed as

$$\begin{aligned}\frac{4\mu}{\sqrt{r/2\pi}}u_s &= K_I\{\cos\phi\,[(2\gamma-1)\cos\theta/2-\cos 3\theta/2] \\ &\quad -\sin\phi\,[(2\gamma+1)\sin\theta/2-\sin 3\theta/2]\} \\ &\quad +K_{II}\{\cos\phi\,[(2\gamma+3)\sin\theta/2+\sin 3\theta/2]\end{aligned}$$

$$+ \sin\phi\,[(2\gamma - 3)\cos\theta/2 + \cos 3\theta/2]\} \tag{45}$$

and

$$\begin{aligned}\frac{4\mu}{\sqrt{r/2\pi}}u_n &= K_I\{\sin\phi\,[(2\gamma-1)\cos\theta/2 - \cos 3\theta/2] \\ &\quad + \cos\phi\,[(2\gamma+1)\sin\theta/2 - \sin 3\theta/2]\} \\ &\quad + K_{II}\{\sin\phi\,[(2\gamma+3)\sin\theta/2 + \sin 3\theta/2] \\ &\quad - \cos\phi\,[(2\gamma-3)\cos\theta/2 + \cos 3\theta/2]\}\end{aligned} \tag{46}$$

where (r,θ) are the polar coordinates centered at the crack-tip and ϕ is the inclination of the crack to x-axis. The parameter γ is defined as:

$$\gamma = \begin{cases} (3-4\nu) & (plane-strain) \\ (3-\nu)/(1+\nu) & (plane-stress) \end{cases} \tag{47}$$

Chan, Tuba and Wilson [9] applied the conventional finite element technique to determine the stress intensity factors at crack tips. However, a very substantial refinement of the finite element mesh around the crack tip was required. An accurate value of the stress intensity factor can be obtained by the quarter-point element such as Henshell and Shaw [10] and Barsoum [11]. The special enriched element with the values of K_I and K_{II} included in the solution was first formulated by Benzley [12] and then extended by Gifford and Hilton [13]. Another group of researchers such as Tong, Pian and Lasry [14], Atluri, Kobayashi and Nakagaki [15] and Lin and Mar [16] applied the hybrid element approach to obtain the stress intensity factors.

In this study, the quarter-point element (QPE) is applied to determine the stress intensity factors. The QPE can reproduce the $\sqrt{r}$ type displacement variation in the vicinity of a crack-tip (as given by (45) or (46)). This is achieved by placing the mid-nodes adjacent to the crack-tip node at the quarter positions as shown in Figure (2). In this case, the corrected order of stress singularity can be reproduced. Also, the full convergence and conformity of the elements are preserved. In order to use QPE efficiently, the following considerations should be observed:

(i) the size of the QPE relative to the crack length (15% to 25%),

(ii) the number of QPEs enclosing the crack-tip should be at least five, and

(iii) the use of proper transition element's size.

The article by Murti and Vallippan [17] provides further guidelines to the considerations (i) to (iii). The numerical value obtained by an efficient use of QPE should be within an error bound of 5%.

Using the QPE, the stress intensity factor can be evaluated by the nodal displacements along rays emanating from the crack-tip and by equating the coefficients of $\sqrt{r}$ in (45) or (46). For $\phi = 0°$,

$$K_I \left\{ \begin{array}{c} (2\gamma - 1)\cos\theta/2 - \cos 3\theta/2 \\ (2\gamma + 1)\sin\theta/2 - \sin 3\theta/2 \end{array} \right\} = \frac{4\mu}{\sqrt{\ell_i/2\pi}} \left\{ \begin{array}{c} 4u_{x2} - u_{x3} - 3u_{x1} \\ 4u_{y2} - u_{y3} - 3u_{y1} \end{array} \right\} \tag{48}$$

and

$$K_{II} \left\{ \begin{array}{c} -(2\gamma + 3)\sin\theta/2 - \sin 3\theta/2 \\ (2\gamma - 3)\cos\theta/2 + \cos 3\theta/2 \end{array} \right\} = \frac{4\mu}{\sqrt{\ell_i/2\pi}} \left\{ \begin{array}{c} 4u_{x2} - u_{x3} - 3u_{x1} \\ 4u_{y2} - u_{y3} - 3u_{y1} \end{array} \right\} \tag{49}$$

with $\ell_i = \ell_1$ or ℓ_2 defined in Figure (2). When $\theta = 0°$ or $180°$, the stress intensity factors must be evaluated by the non-zero component from either (48) or (49).

6 MODELLING OF LOW-TEMPERATURE-INDUCED FAILURE

In this section we consider the problem of a typical pavement structure which is composed of an asphalt pavement underlain by a compacted base (Figure 3). The thermo-mechanical properties of the asphalt, the base and the underlying soil are characterized by the shear modulus (G), Poisson's ratio (ν), the thermal conductivity (k), heat capacity (ρc) and the coefficient of thermal expansion/contraction (α). The tensile strength of the asphalt layer is denoted by σ_o. In the ambient state temperature distribution within the pavement and the underlying strata are assumed to be at a constant value (T_o). (It is appreciated that this is an approximation, since, in practice a thermal gradient can exist within the pavement structure, consistent with the heat transfer characteristics of its components and the heat supply/loss from the subsoils). In this study, the entire surface of the asphalt pavement is subjected to a step function of temperature reduction. The thermal jump is denoted by $\mid T^* - T_o \mid$. Where T_o is the initial temperature within the pavement structure and T^* is the new value of the surface temperature associated with the thermal jump. Since the problem displays symmetry in terms of the thermal loading, attention is restricted to the thermo-elastic analysis of a one-dimensional element which is constrained in the horizontal direction. The time discretization is used to solve the transient effects and the failure condition $\sigma_{zz}(x,t) = \sigma_o$ is used to establish, incrementally, the extent of the failure zone. In the failed region the tractions are set equal to zero. The Figure (4) illustrates the progression of the failure zone within the asphalt layer, with time. The results indicate the influence of the tensile strength-stiffness ratio of the asphalt layer on the extent of the failure region.

7 MODELLING OF LOW-TEMPERATURE-INDUCED FRACTURE - EFFECT OF A REINFORCING LAYER

In this section we examine the influence of a reinforcing layer on the low temperature induced fracture propagation potential. The typical pavement structure considered in this phase of the study is a cracked pavement which rests on a compacted subgrade. For purposes of the simplification of the analysis attention is restricted to the case where the compacted based is considered to be rigid. A reinforcing layer is placed at the interface between the existing pavement and the overlay at the cracked location. The objective of the study is to examine the potential for the propagation of the crack into the new overlay and the ability of the reinforcing layer to suppress such crack propagation. The reduction in the stress intensity factor (flaw opening mode) is interpreted as a inhibition to crack propagation into the overlay. The thermomechanical properties of the two asphalt layers are characterized by $\mu_i(G_i)$, ν_i, k_i, $(\rho c)_i$ and α_i where $i = 1$, and 2 refer to the asphalt overlay and the existing cracked pavement respectively. The stiffness of the reinforcing layer is defined by the parameters EA. The thickness of the asphalt overlay and the cracked pavement are denoted by h_1 and h_2 respectively. In order to examine the influence of the potential for reflection of the crack we assume that the crack extends beyond the reinforcement over a distance ℓ. The potential for the suppression of crack propagation during low temperature effects is addressed by examining the flaw opening mode stress intensity factor at this crack tip. It should be noted that in this study the compacted base is considered to be rigid. Consequently, it is important to clearly identify the mode of interaction between the asphalt layer 2 and the rigid base.

Case 1: The asphalt layer exhibits complete bonding with the compacted base.

Case 2: The asphalt layer-compacted base interface is partially bonded and frictionless in the unbonded regions.

Case 3: The interface between the asphalt layer and the compacted base is frictionless and bi-lateral.

In all the three cases, the surface of the pavement is subjected to a step function of temperature reduction. The thermal jump is defined by $T = \mid T^* - T_o \mid$. The transient finite element analysis is applied to study the problem and the stress intensity factor is evaluated by the procedure given in section 5. A typical time-dependent stress intensity factor for the opening mode can shown in Figure (5). In cases (1) to (3), the parameter B indicates the extent of the frictionless region at the asphalt layer-compact base interface. That is $B/h_1 = 0$ for case (1): $B/h_1 = 2.0$ for case (2) and $B/h_1 = \infty$ for case (3). The results relevant for the case (1) are given in Figures (6) to (8). Similar results for the cases (2) and (3) are given in Figures (9) to (14). The following parameters are employed in the

numerical simulations: $h_1/h_2 = 0.5$; $\Gamma = (\alpha_1 G_1/\alpha_2 G_2)$=0.1, 0.2, 1.0 and 10.0; ℓ/h_1 =0.25, 0.50 and 0.75 and $G_1 = G_2$. Each curve in the Figures (6) to (14) indicate the effect of the stiffness of the reinforcement on the stress intensity factor for the crack opening mode. A considerable reduction of the stress intensity factor can be achieved by increasing the stiffness of the reinforcement.

8 MODELLING OF LOW-TEMPERATURE-INDUCED FRACTURE - EFFECT OF INTERFACE CHARACTERISTICS

In this section we focus on the category of problem in which different types of interface conditions are incorporated at the interface between the asphalt layer and the compacted base and the compacted base and the underlying subgrade soil. The thermomechanical properties of the asphalt layer, the compacted base and the subgrade are characterized by the elastic and thermal material parameters μ_i, ν_i, k_i $(\rho c)_i$, and α_i where i=1,2,3 refer to the asphalt layer, the compacted base and the subgrade, respectively. The thickness of the aforementioned components of the pavement structure are also denoted by h_i. The study examines the influence of interface conditions by appeal to two basic models of cracked pavement. One model refers to the situation where surface cracks are present in the pavement structure in a periodic fashion (cases 1, 3, 5, 7 and 9). The second model examines the pavement structure in which deep cracks extend in a periodic fashion, well beyond the compacted base (cases 2, 4, 6, 8, 10). These categories of pavement structures are illustrated in Figure (15). The interface conditions between the various components of the pavement structure are classified as follows:

(a) Bonded Interface: In the case of bonded interface complete continuity of the displacements and the stresses are maintained across the interface.

(b) Frictionless Contact: Interface with the continuity of the vertical displacement and the vertical traction across the interface are maintained. The corresponding displacement and the traction in the horizontal direction are independent across the interface. In this case, double nodes are required on each side of the interface and they are connected by a special interface element discussed in section (3.2). It is assumed that due to the self weight stresses the contact at the frictionless interface is maintained without separation.

(c) Frictionless Interface With Separation: The continuity conditions for the displacement and traction are identical to those in (b). Under low temperature conditions, tensile stresses can be induced across the interface. In (b), it is assumed that the self weight effects are sufficient to maintain contact between the various layers. In this case, however, the actual self weight stresses are considered and separation allowed to occur in regions of the interface where the temperature induced normal stresses at the interface exceed the self weight stresses. In the finite element analysis, the region of separation at the interface location has to be determined by using the iterative technique discussed in section (4).

It is assumed that the pavement structures exhibit a uniform initial temperature (T_o) within all its elements. The surface of the pavement is subjected to a step function of

temperature reduction. The thermal jump is defined by $T = \mid T^* - T_o \mid$. The transient finite element analysis is used to evaluate the stress intensity factors for the crack opening mode at the surface crack tip. The specific time-dependent variations in the stress intensity factor K_I are given in Figures (16) and (17). In the specific numerical computations the following parameters are considered: $h_2/h_1 = 3.0$, $h_3/h_1 = 30.0$ and ℓ/h_1=0.2, 0.4, 0.6 and 0.8. The Table I summarizes the basic features of cracking pattern and bond conditions examined in the problems treated in this section.

The Figures (18) to (21) illustrate the parametric variation of the flaw opening mode stress intensity factor at a surface flaw in a layered system for bonding conditions at the various interfaces, the isolation effect of cracking patterns and the thermo-elastic mismatch between the asphalt layer and the compacted base.

9 CONCLUSIONS

This report examines the modelling of the low temperature thermo-mechanical performance of a pavement structure by appeal to a transient thermoelastic analysis. The linear thermoelastic modelling of the pavement response is intended to provide a first approximation to the more complicated time and temperature dependent mechanical behaviour of the pavement material. The finite element modelling is used to examine a number of plausible situations pertaining to either the fracture initiation or fracture propagation of typical pavement structures and overlays which incorporate reinforcing layers. The basic findings of the study can be summarized as follows:

(a) The surface temperature fluctuations generate stresses in the various layers of a pavement structure. In the case of an undamaged pavement the transient thermoelastic analysis coupled with an elementary failure criterion can be used to assess the conditions that promote failure in the asphalt layer.

(b) The transient thermoelastic finite element analysis can be combined with a crack model to examine the influenced of low temperature effects on the propagation of existing flaws in the pavement structure.

(c) When the temperatures of the asphalt surface are lowered the stress intensity factors at surface flaws that are present in the asphalt layer experience a corresponding increase. In situations where a series of cracks of different crack lengths are present in the asphalt layer, the dominant cracks will tend to propagate first. In general, when the dominant cracks are extended the tendency for propagation of other surface cracks can be relieved.

(d) The tendency for the propagation of an existing flaw is characterized by the amplification of the stress intensity factor at the flaw boundary. It is observed that the low temperature induced flaw opening mode stress intensity factor is influenced by among others, the flaw size and frequency, the thermal and elastic mismatch between the various layers comprising the pavement and the extent of delamination between the layers.

(e) The propensity for propagation of surface flaws in an asphalt layer due to low temperature effects can be related to the "the isoelastic mismatch parameters" which can be defined by the ratio $\alpha_1\mu_1/\alpha_2\mu_2$ where α_i are the coefficients of thermal contraction and μ_i the shear moduli and $i = 1$ corresponds to the asphalt layer and $i = 2$ corresponds to the base layer. In general, the tendency for crack propagation can be increased by an increase in the thermoelastic mismatch between the two layers.

(f) The incorporation of a fully extended reinforcing layer between a cracked pavement and a newly placed fully bonded overlay will tend to reduce the extension of the

crack into the new overlay. The effectiveness of the reinforcement can be assessed by appeal to the thermoeleastic mismatch parameter and a relative stiffness parameter which relates the extensional stiffness of the reinforcement to the deformability characteristics of the surface layer and its thickness. Suitable combinations of the thermoelastic mismatch parameter and the relative stiffness parameter can yield the optimum efficiency of the reinforcing action.

10 REFERENCES

[1] Design Techniques to Minimize Low-Temperature Asphalt Pavement Transverse Cracking, The Asphalt Institute Research Report, No.81-1, RR-81-1 (1981).

[2] Paving in Cold Areas, Proceedings of the Mini-Workshop, Canada/Japan Science and Technology Consultations, Vancouver, B.C., Vol.1 and 2 (1982).

[3] Proceedings of Paving in Cold Areas, Mini-Workshop, Canada/Japan Science and Technology Consultations, Tsukuba, Japan (1984).

[4] Sugawara, T., Kubo, H. and Moriyoshi, A., Low Temperature Cracking of Asphalt Pavements, Paving in Cold Areas, Proceedings of Canada/Japan Science and Technology Consultations, Vancouver, B.C., Vol.1, 3-42 (1982).

[5] Kovalenko, A.D., Thermoelasticity, Wolters-Noordhoff Publishing Co., Groningen, The Netherlands (1969).

[6] Carlson, D.E., Linear Thermoelasticity in Mechanics of Solids II, Handbuch der Physik, (S. Flugge, Ed.) Springer-Verlag, Berlin, 297-345 (1972).

[7] Zienkiewicz, O.C., The Finite Element Method in Engineering Science, McGraw-Hill, New York, (1977).

[8] Sih, G.C. and Liewbowitz, H., Mathematical Theories of Brittle Fracture. In Fracture (Ed. H. Liebowitz), Vol.II, 67-190, Academic Press, New York, (1968).

[9] Chan, S.K., Tuba, I.S. and Wilson, W.K., On Finite Element Method in Linear Fracture Mechanics, Engineering Fracture Mech., 2, 1-17, (1970-71).

[10] Henshell, R.D. and Shaw, K.G., Crack Tip Finite Elements are Unnecessary, Int. J. Numerical Methods in Engineering, 9, 495-507 (1975).

[11] Barsoum, R.S. On the Use of Isoparametric Finite Elements in Linear Fracture Mechanics, Int. J. Numerical Methods in Engineering, 10, 25-37 (1976).

[12] Benzley, S.F., Representation of Singularities With Isoparametric Finite Elements, Int. J. for Numerical Methods in Engineering, 8, 537-545 (1974).

[13] Gifford, L.N. and Hilton, P.D., Stress Intensity Factors By Enriched Finite Elements, J. Eng. Fracture Mech., 10, 485-496 (1978).

[14] Tong, P., Pian, T.H.H. and Lasry, S.J., A Hybrid-Element Approach to Crack Problems in Plane Elasticity, Int. J. for Numerical Methods in Engineering, 7, 297-308 (1973).

[15] Atluri, S.N., Kobayashi, A.S. and Nakagaki, M., An Assumed Displacement Hybrid Finite Element Model for Linear Fracture Mechanics, Int. J. Fracture, II, 257-271 (1975).

[16] Lin, K.Y. and Mar, J.W., Finite Element Analysis of a Stress Intensity Factor for Cracks at a Bi-Material Interface, Int. J. Fracture, 12, 521-531 (1976).

[17] Murti, V. and Valliappan, S., A Universal Optimum Quarter Point Element, Engineering Fracture Mech., 25, 237-258 (1986).

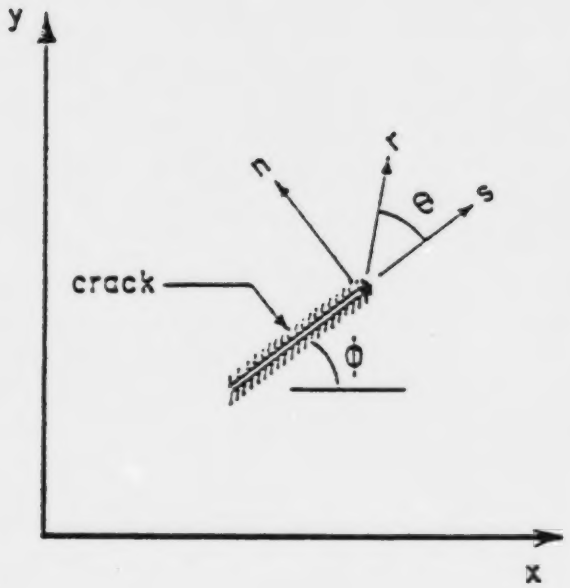

Figure 1: The Local Coordinate System at the Crack Tip

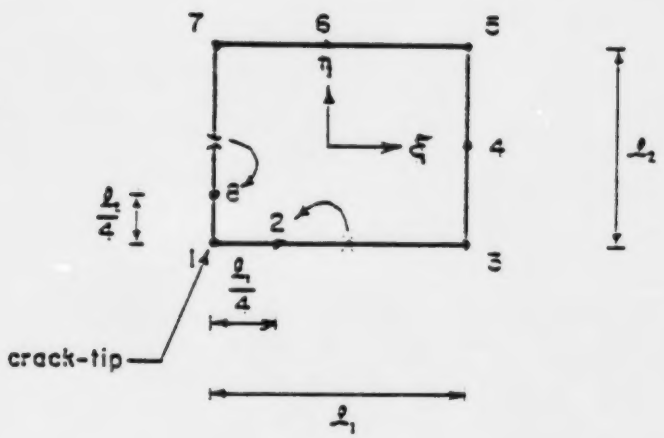

Figure 2: The Quarter-Point Element

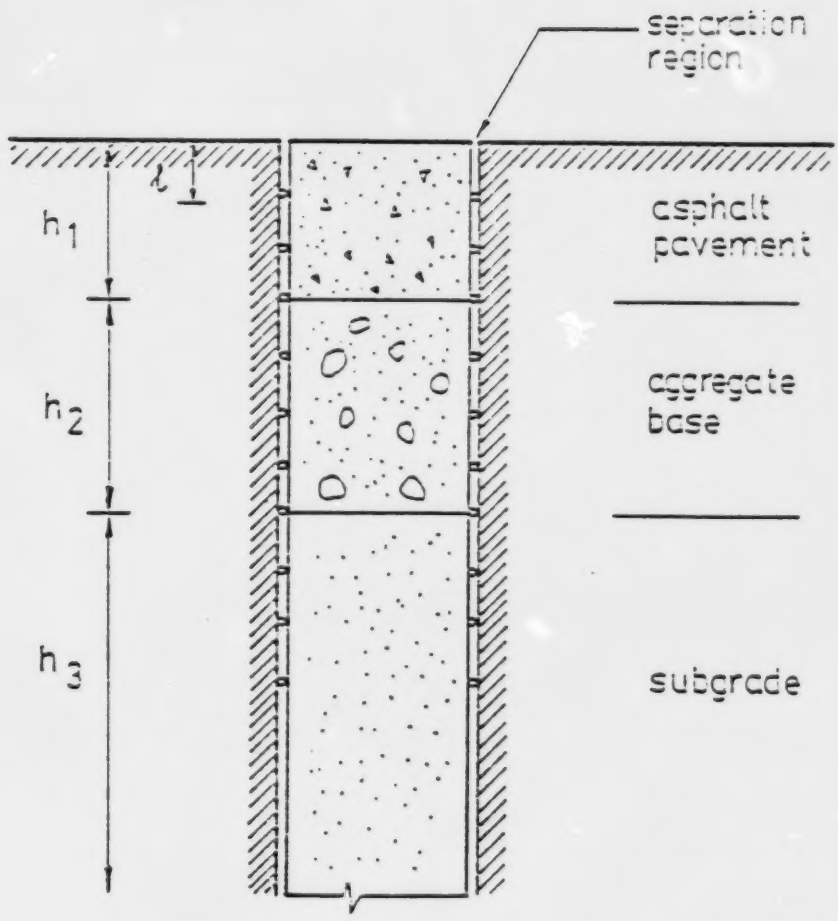

Figure 3: Geometry of the Pavement Structure

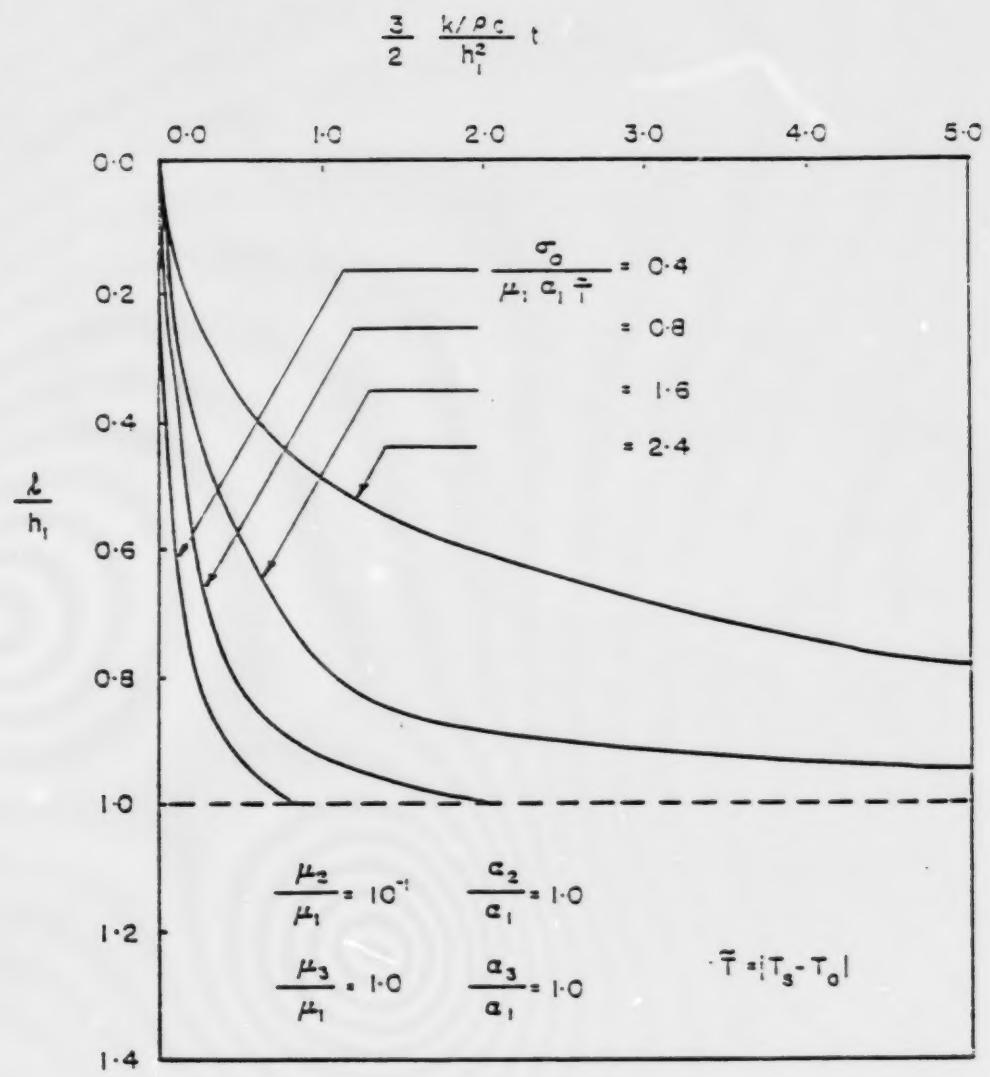

Figure 4: Time-Dependent Generation of Failure Within the Asphalt Layer: Influence of a Temperature Decrease at the Surface

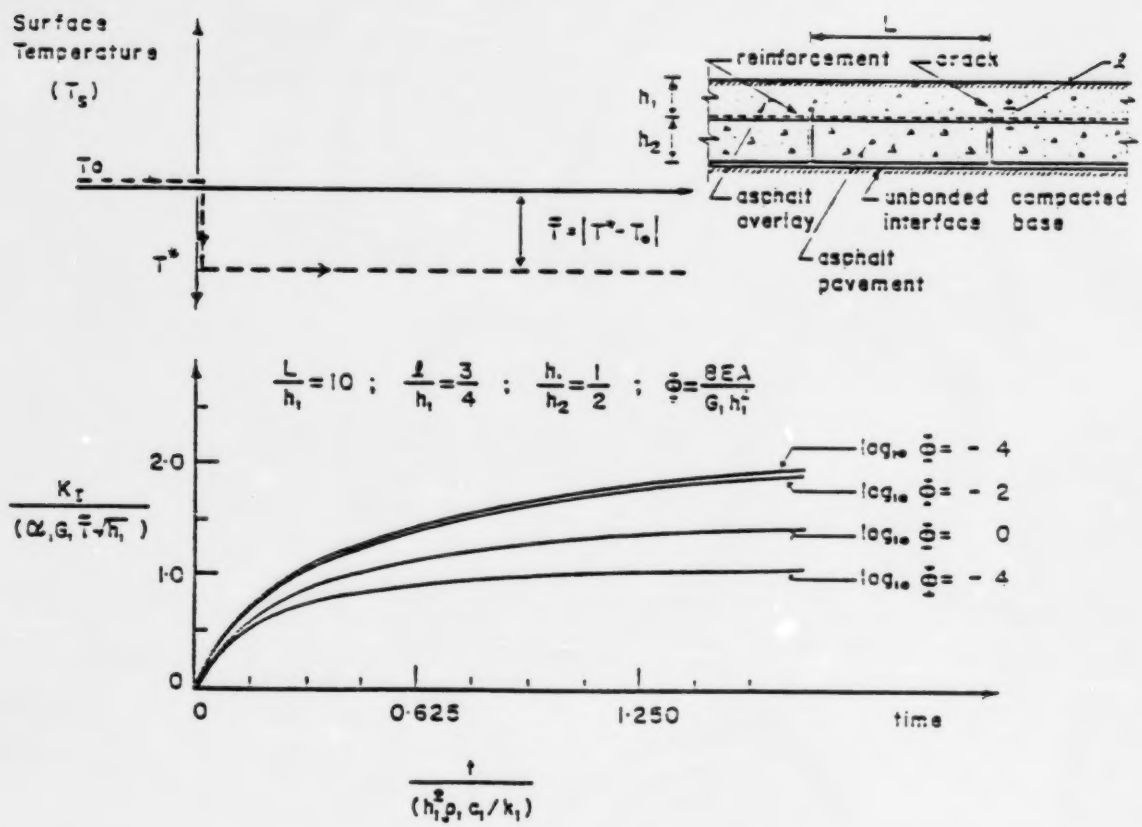

Figure 5: The Time-Dependent Variation of the Stress Intensity Factor at the Crack Tip: Influence of a Reinforcing Layer

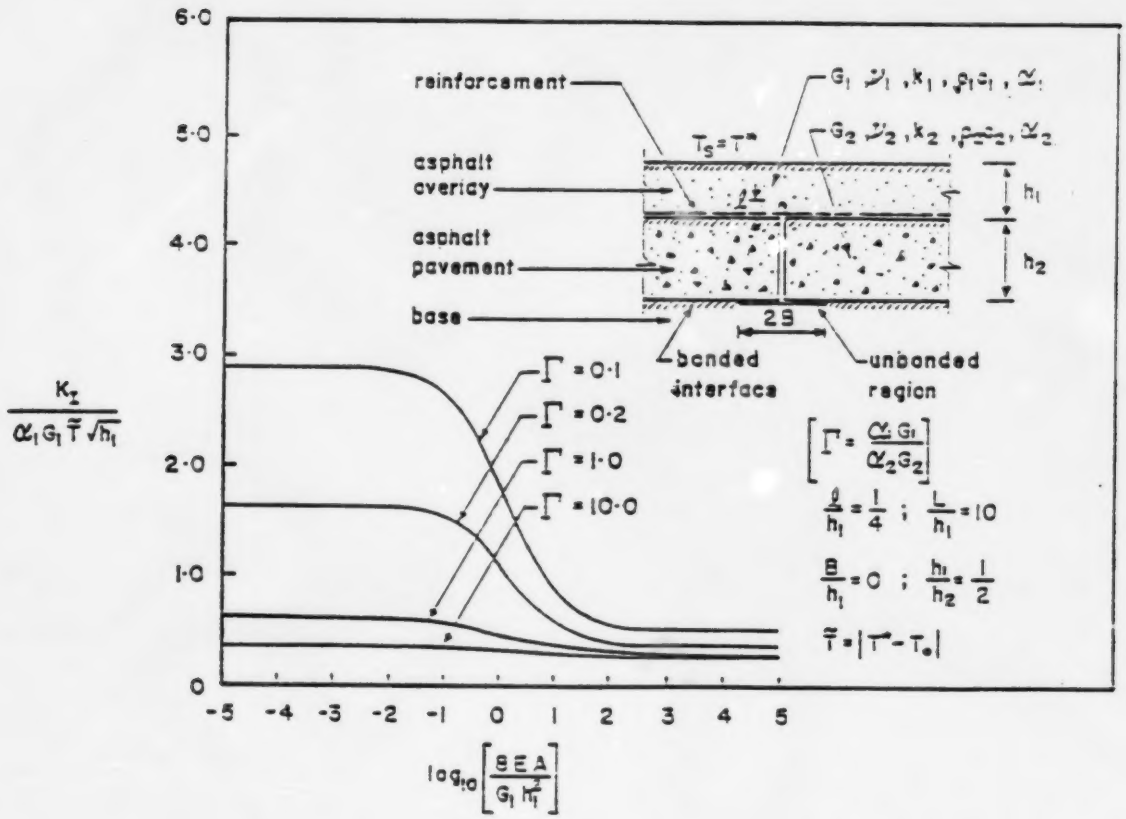

Figure 6: The Influence of a Reinforcing Layer on the Stress Intensity Factor at an Extended Crack Tip (Case 1)

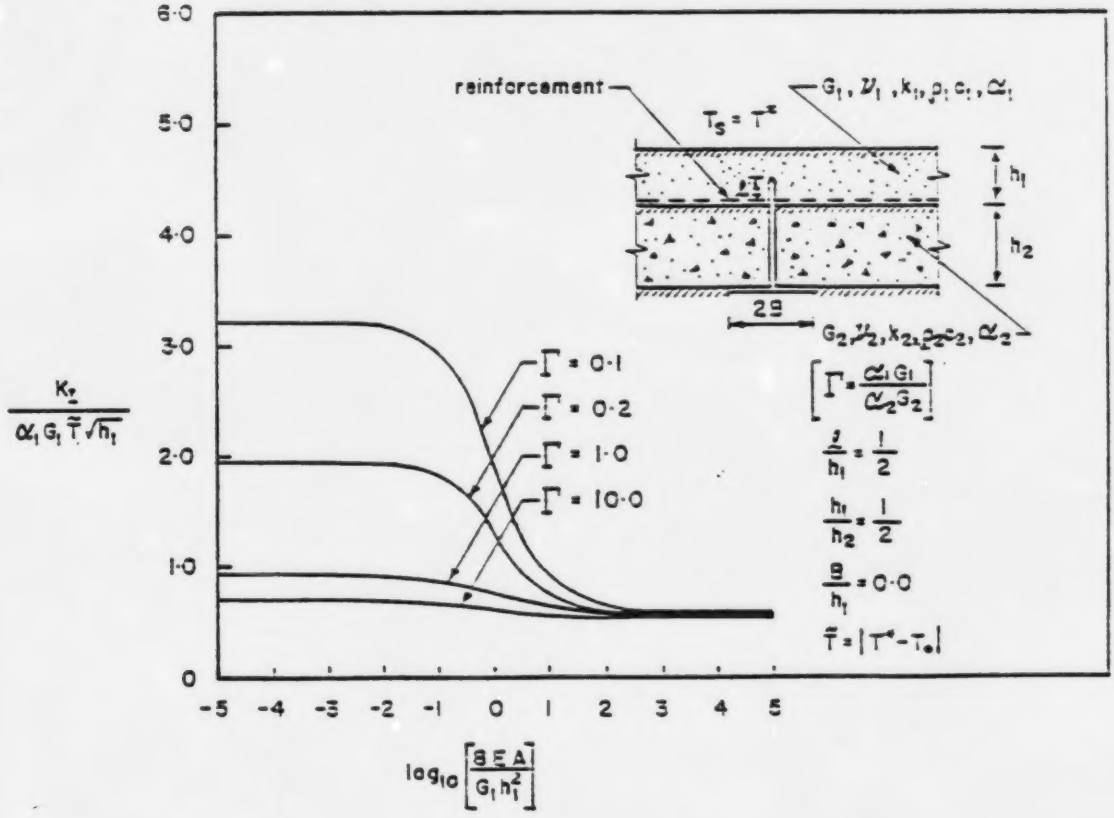

Figure 7: The Influence of a Reinforcing Layer on the Stress Intensity Factor at an Extended Crack Tip (Case 1)

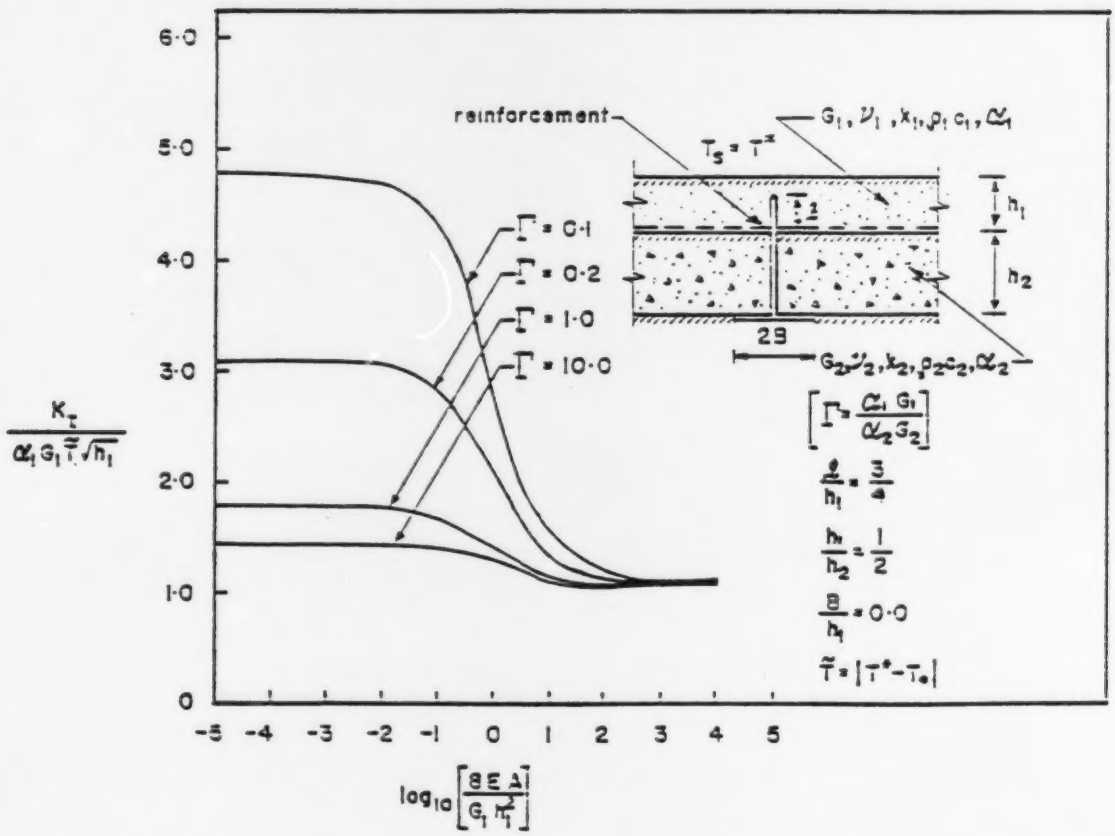

Figure 8: The Influence of a Reinforcing Layer on the Stress Intensity Factor at an Extended Crack Tip (Case 1)

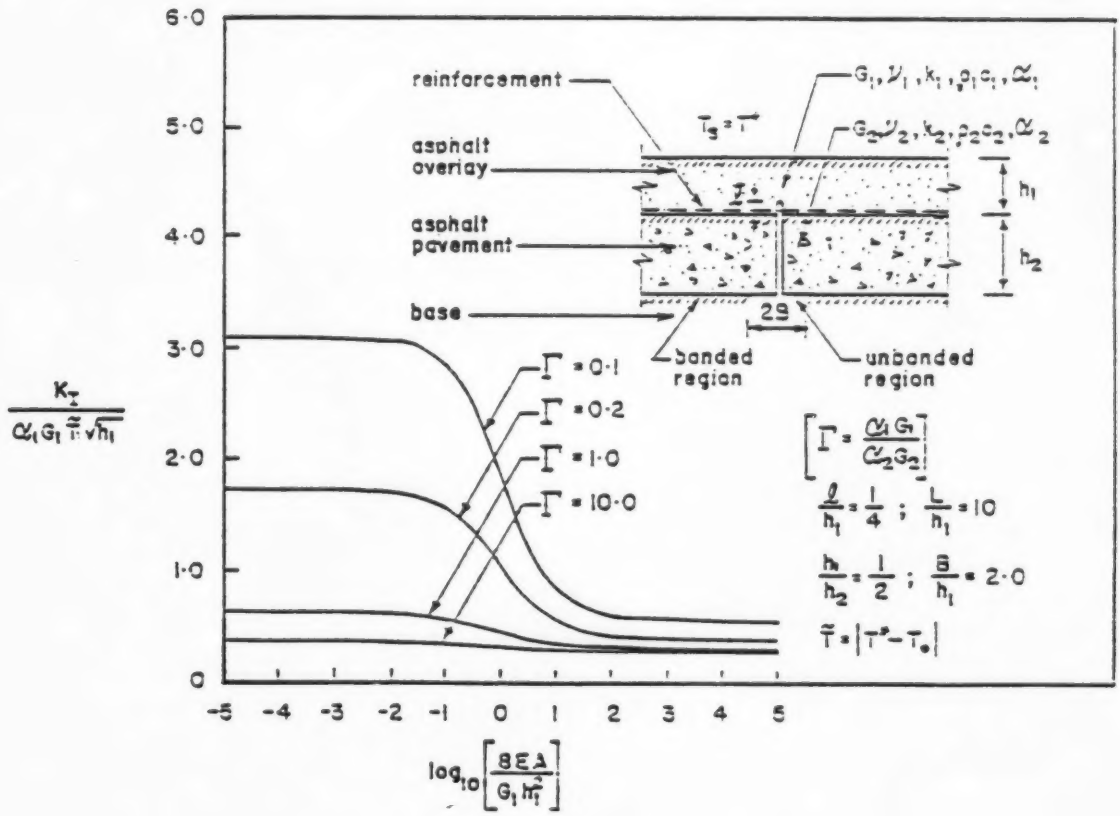

Figure 9: The Influence of a Reinforcing Layer on the Stress Intensity Factor at an Extended Crack Tip (Case 2)

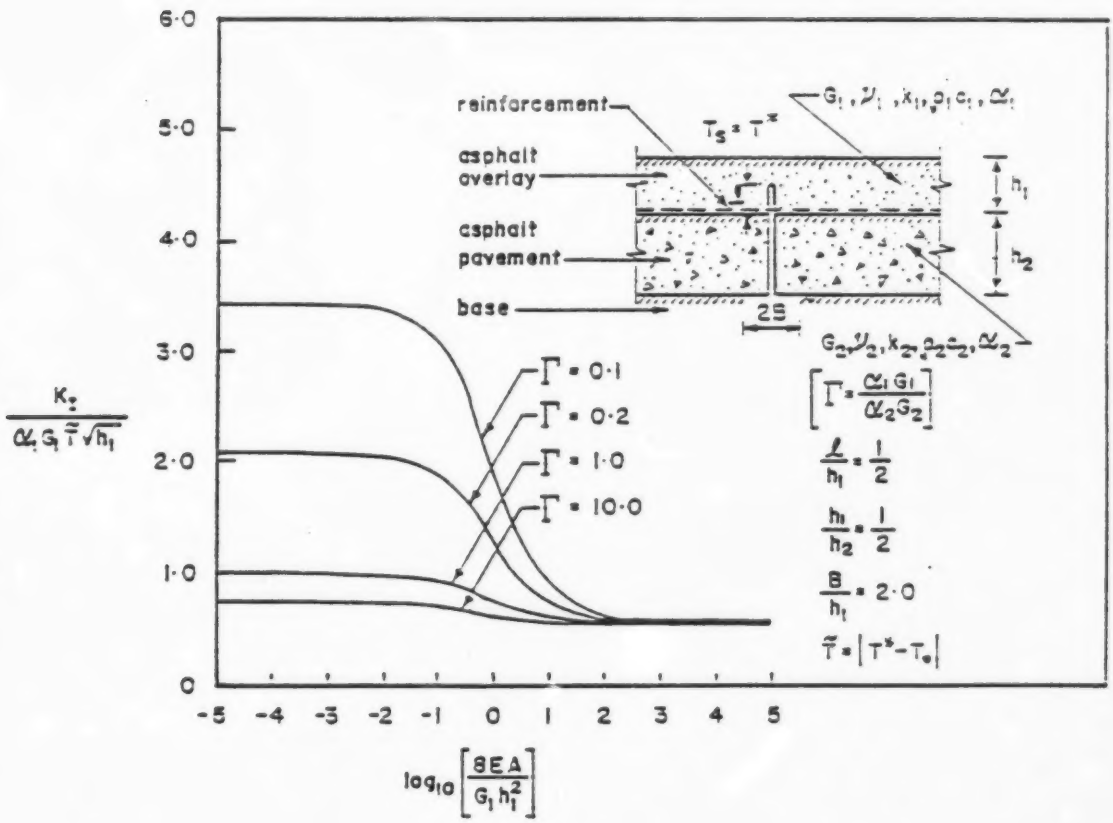

Figure 10: The Influence of a Reinforcing Layer on the Stress Intensity Factor at an Extended Crack Tip (Case 2)

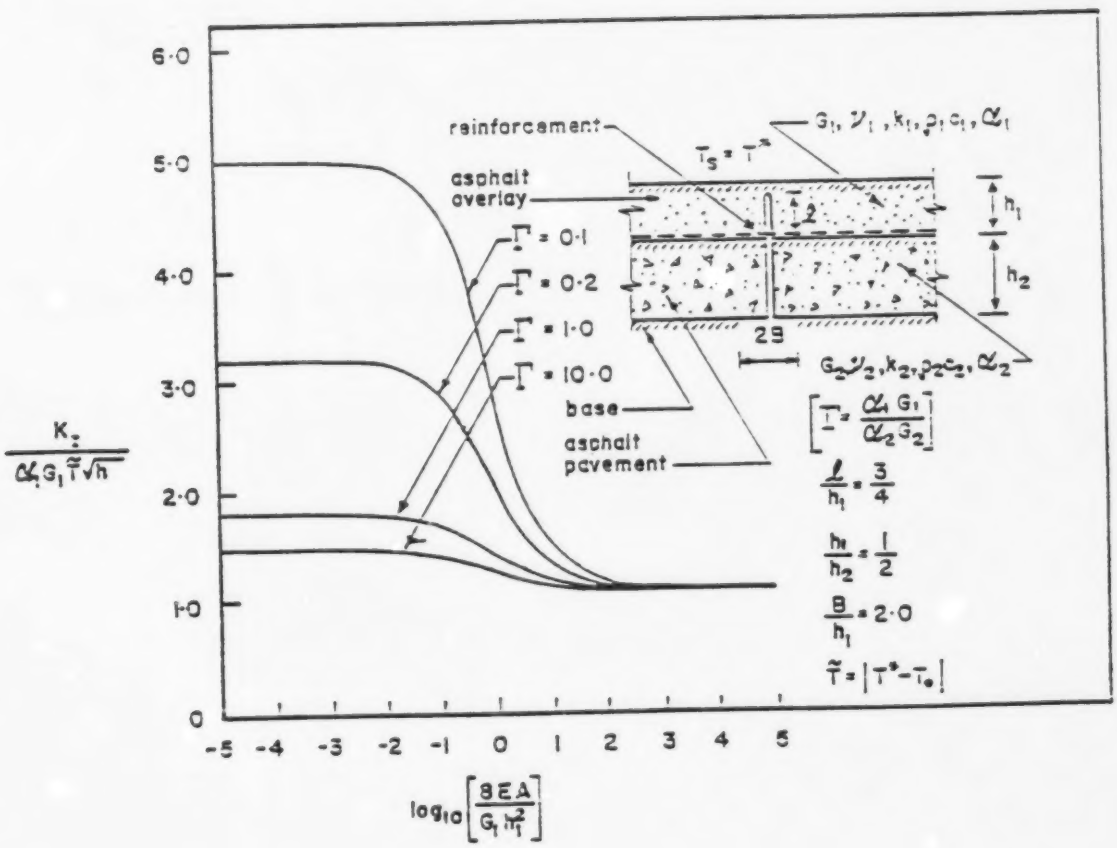

Figure 11: The Influence of a Reinforcing Layer on the Stress Intensity Factor at an Extended Crack Tip (Case 2)

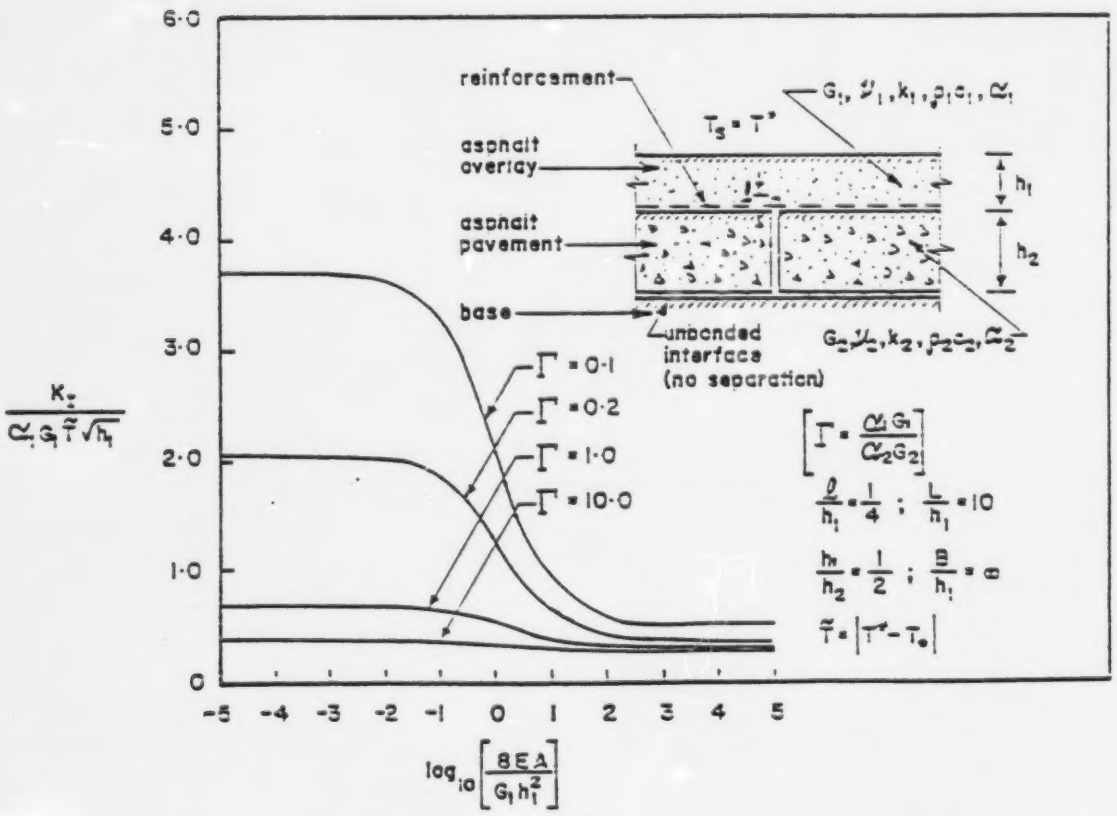

Figure 12: The Influenced of a Reinforcing Layer on the Stress Intensity Factor at an Extended Crack Tip (Case 3)

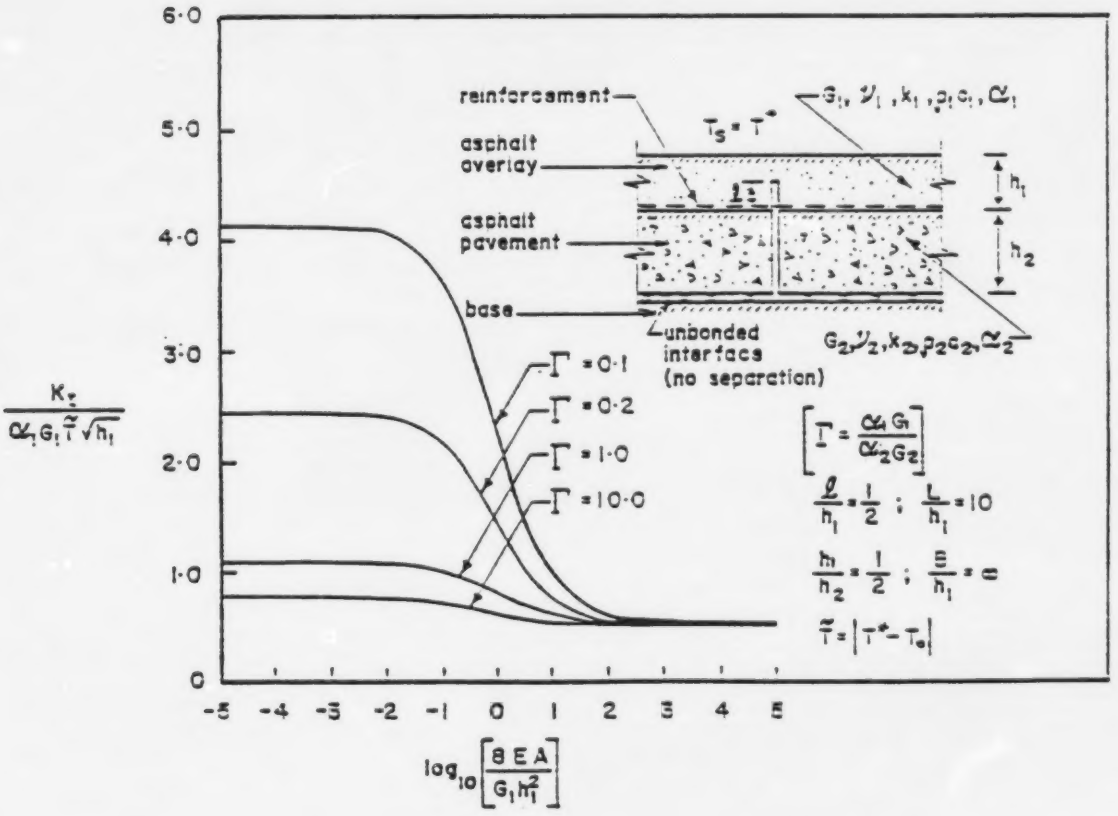

Figure 13: The Influenced of a Reinforcing Layer on the Stress Intensity Factor at an Extended Crack Tip (Case 3)

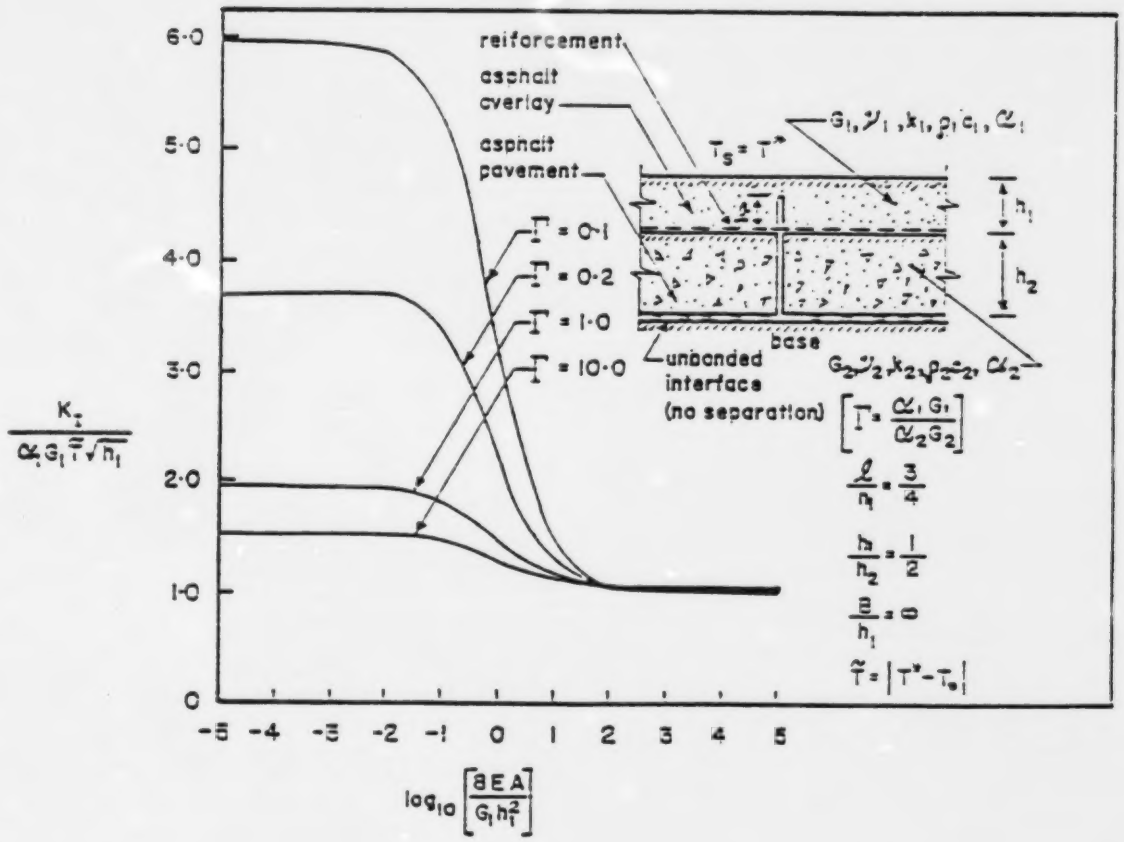

Figure 14: The Influenced of a Reinforcing Layer on the Stress Intensity Factor at an Extended Crack Tip (Case 3)

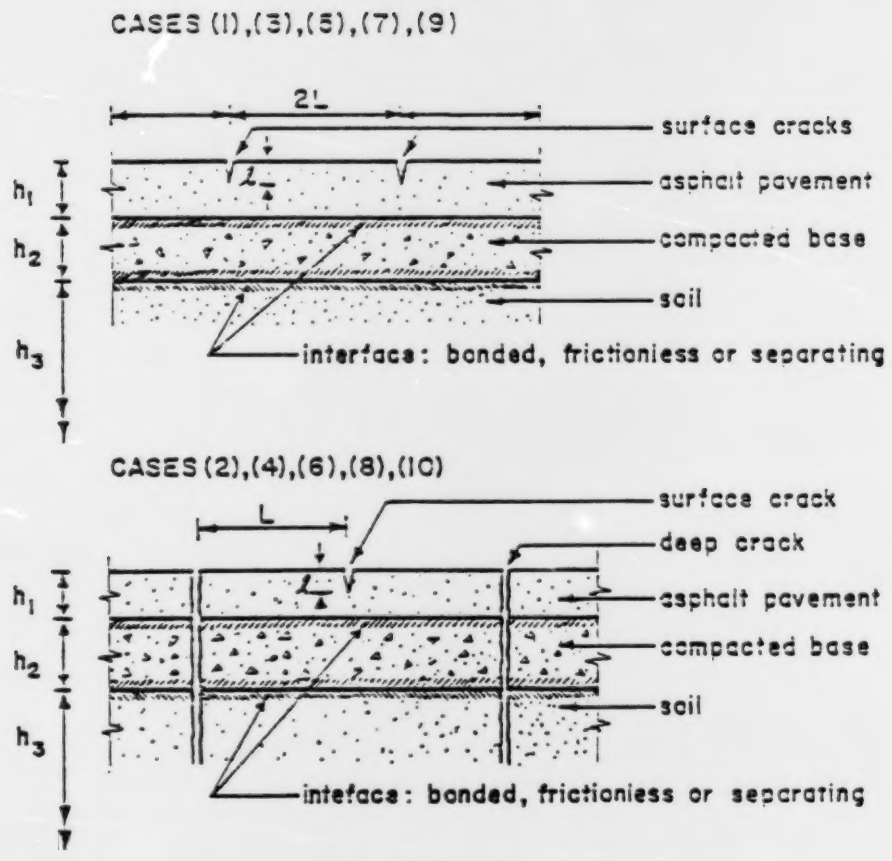

Figure 15: Modelliing of Low Temperature Induced Fracture: Effects of Debonding and Separation

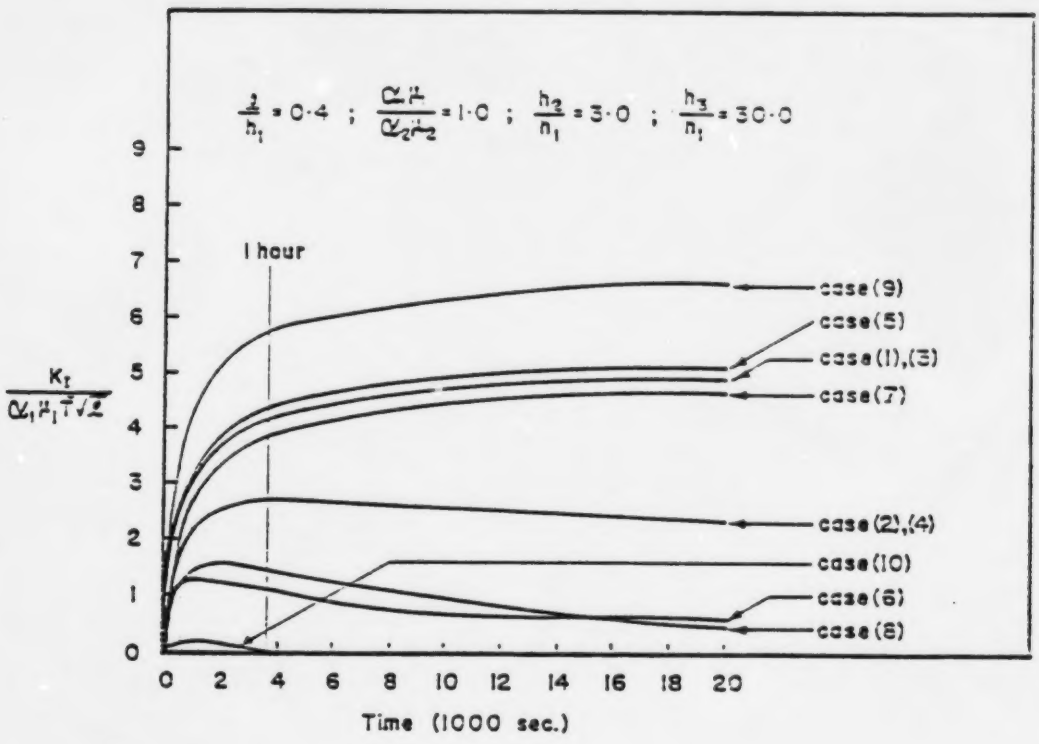
$\frac{d}{h_1} = 0.4$; $\frac{\alpha_1 \mu_1}{\alpha_2 \mu_2} = 1.0$; $\frac{h_2}{h_1} = 3.0$; $\frac{h_3}{h_1} = 30.0$
1 hour
case (9)
case (5)
case (1), (3)
case (7)
case (2), (4)
case (10)
case (6)
case (8)
$\frac{K_I}{\alpha_1 \mu_1 \sqrt{\ell}}$
0 1 2 3 4 5 6 7 8 9
0 2 4 6 8 10 12 14 16 18 20
Time (1000 sec.)

Figure 16: The Time-Dependent Variations of the Stress Intensity Factor at the Crack Tip: Effects of Debonding and Separation

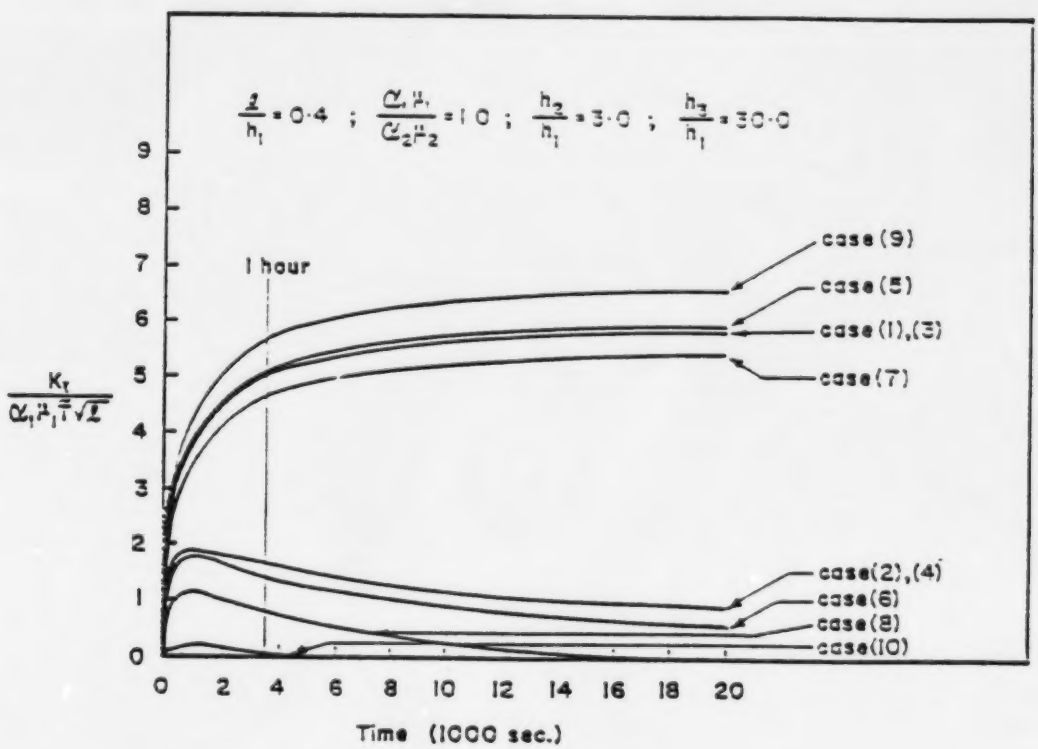

Figure 17: The Time-Dependent Variations of the Stress Intensity Factor at the Crack Tip: Effects of Debonding and Separation

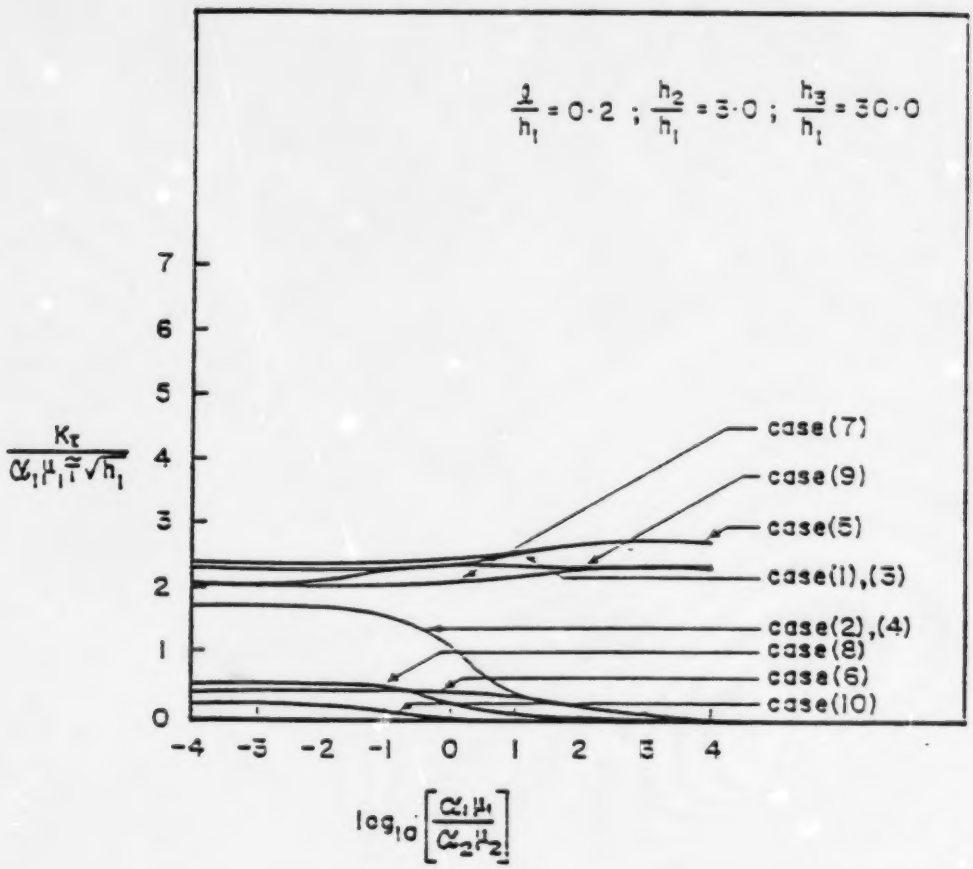

Figure 18: The Variation of the Steady State Stress Intensity Factor With the Thermoelastic Mismatch Parameters $\alpha_1\mu_1/\alpha_2\mu_2$: Effect of Debonding and Separation

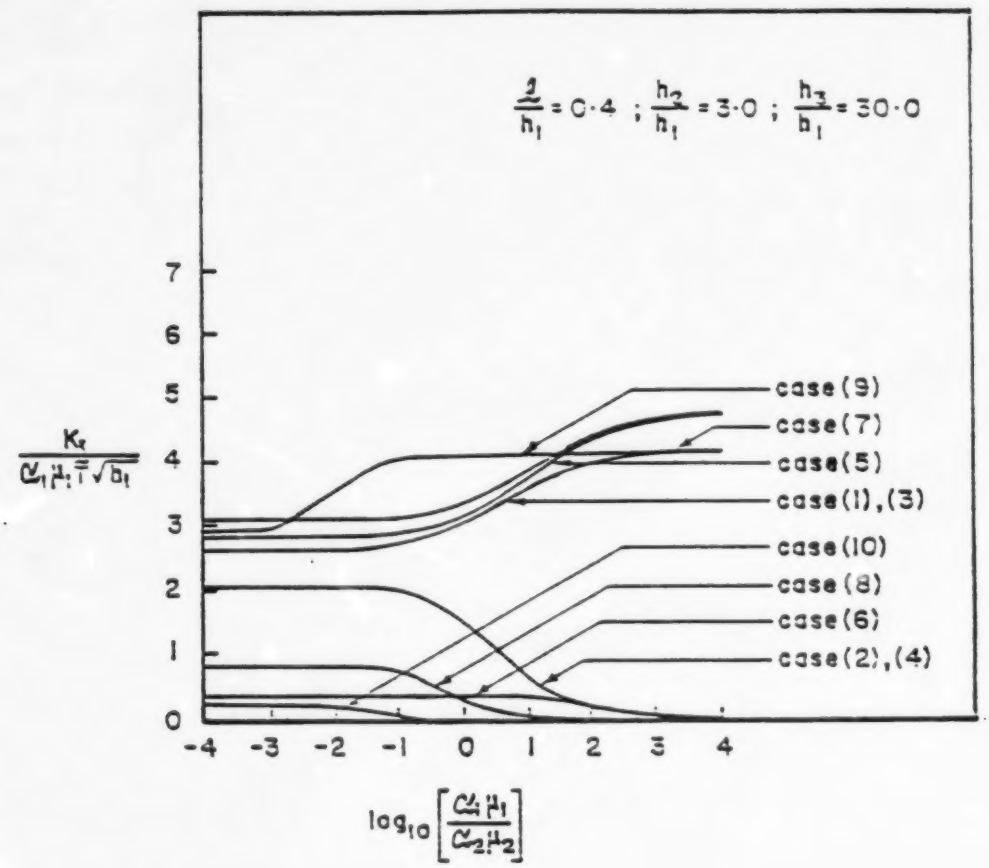

Figure 19: The Variation of the Steady State Stress Intensity Factor With the Thermoelastic Mismatch Parameters $\alpha_1\mu_1/\alpha_2\mu_2$: Effect of Debonding and Separation

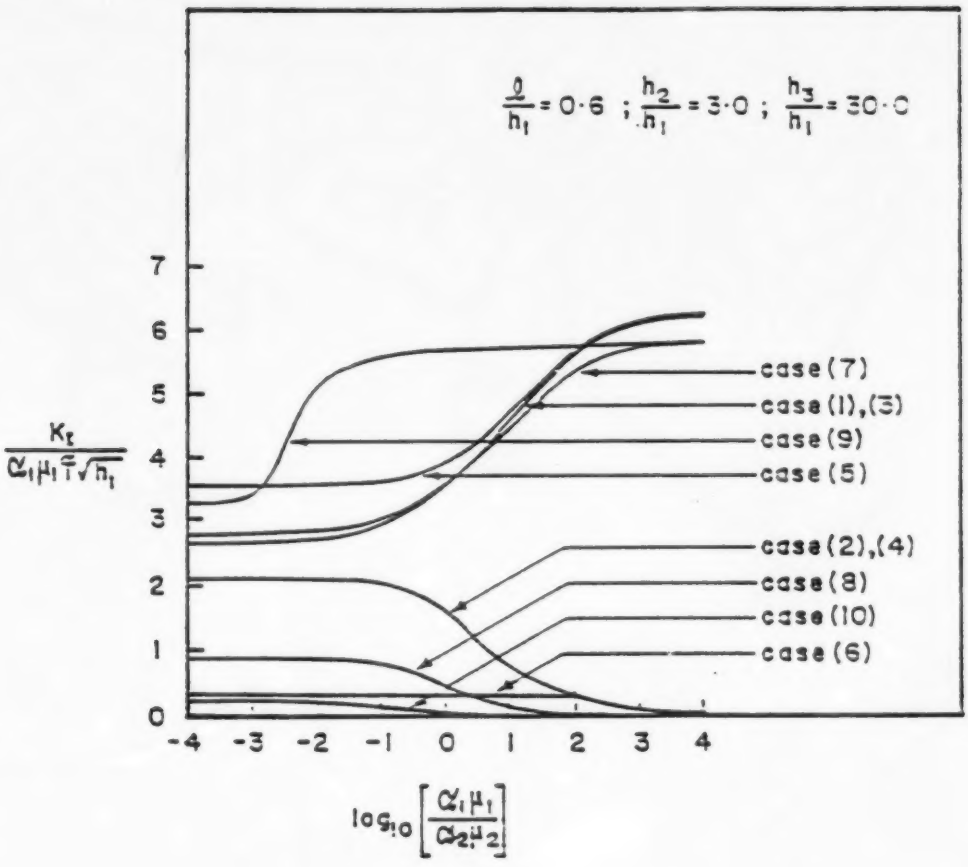

Figure 20: The Variation of the Steady State Stress Intensity Factor With the Thermoelastic Mismatch Parameters $\alpha_1\mu_1/\alpha_2\mu_2$: Effect of Debonding and Separation

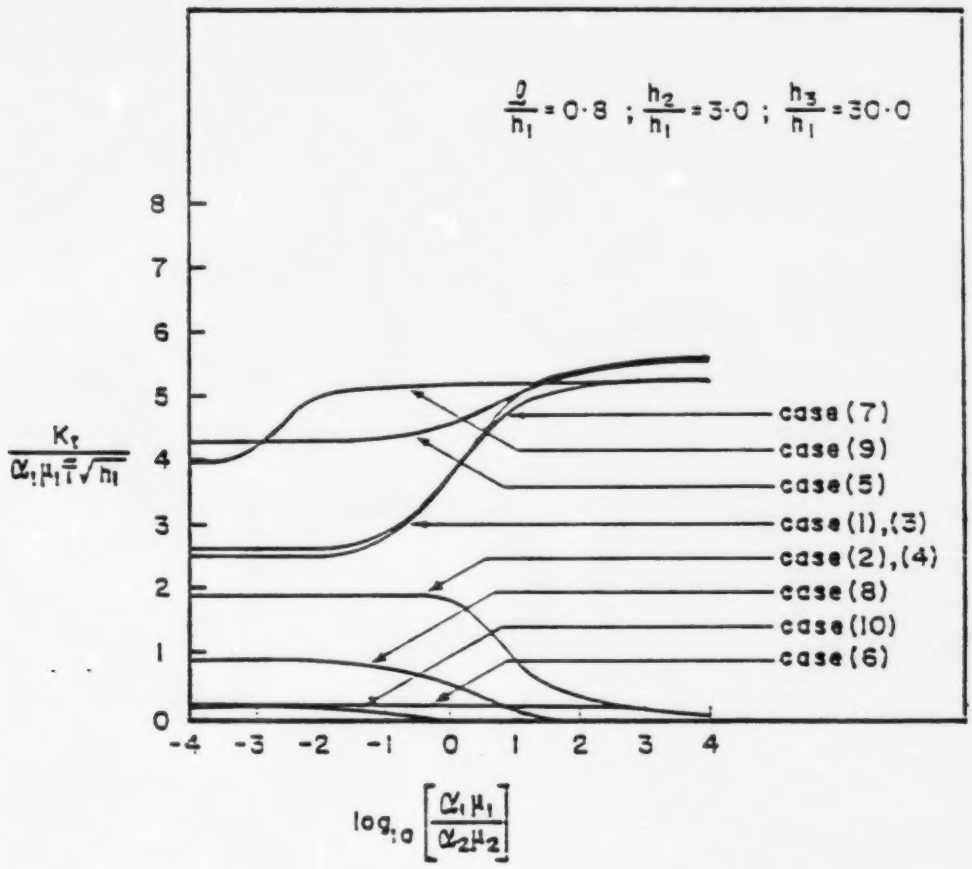

Figure 21: The Variation of the Steady State Stress Intensity Factor With the Thermoelastic Mismatch Parameters $\alpha_1\mu_1/\alpha_2\mu_2$: Effect of Debonding and Separation